

Front propagation in cellular flow

M. Abel¹, A. Celani², D. Vergni^{1,3} and A. Vulpiani^{1,3}

¹ Dipartimento di Fisica, Università di Roma “La Sapienza”, P.le Aldo Moro 2, I-00185 Roma, Italy

² CNRS, INLN, 1361 Route des Lucioles, F-06560 Valbonne, France.

³ INFN, Unità di Roma “La Sapienza”, P.le Aldo Moro 2, I-00185 Roma, Italy

The problem of front propagation in a stirred medium is addressed for flow with cellular patterns. As a consequence of stirring, the effective velocity of the front is enhanced with respect to the non-stirred case. For fast advection the front advances with a velocity proportional to $U^{1/4}$, where U is the stirring intensity, whereas for slow advection the front speed is proportional to $U^{3/4}$. The macroscopic dynamics of the concentration field is described in terms of an effective reaction-diffusion equation with renormalized parameters. The theoretical predictions for the effective front velocity are confirmed by direct numerical simulations.

PACS numbers: 47.27Qb, 47.70Fw

The study of front propagation of a stable phase into an unstable one encompasses several issues of great interest as flame propagation in gases, population dynamics of biological communities (plankton in oceans), chemical reaction fronts in liquids [1]. A common feature of all these phenomena is that they take place in a strongly deformable medium such as a fluid. The interplay among transport, diffusion and reaction is therefore an important issue, with several open problems. In the most compact model of front propagation the state of the system is described by a single scalar field $\theta(t, \mathbf{r})$, which represents the fractional concentration of products. The field θ vanishes in regions of space filled with fresh material (the unstable phase), equals unity where only inert products are left (the stable phase) and takes intermediate values wherever reactants and products coexist, i.e. in the region where production takes place. The evolution of θ is described by the partial differential equation

$$\partial_t \theta + \mathbf{u} \cdot \nabla \theta = \kappa \Delta \theta + \tau^{-1} f(\theta). \quad (1)$$

The second term on the l.h.s. of equation (1) accounts for the transport by an underlying incompressible velocity field [2]. On the r.h.s of (1) the first term describes molecular diffusion and the second one describes the production process, characterized by a typical time-scale τ . We consider a production term of Kolmogorov-Petrovski-Piskunov type [3]. In a medium at rest ($\mathbf{u} = 0$), equation (1) is characterized by a front propagating from, say, left to right, with a speed which reaches the limiting value $v = \sqrt{4\kappa/\tau}$ [4]. In a moving medium, the front propagates with an average limiting speed v_{eff} .

The problem is to determine the dependence of v_{eff} on the typical velocity of the flow U , on its characteristic length-scale L , on the diffusivity κ and on the production time-scale τ . In other words, introducing the Damköhler number $Da = L/(U\tau)$ (the ratio of advective to reactive time-scales) and the Péclet number $Pe = UL/\kappa$ (the ratio of diffusive to advective time-scales), we seek an expression for the enhancement of the front velocity due to advection, as an adimensional function $v_{\text{eff}}/v = \phi(Da, Pe) \geq 1$.

We begin the analysis by stating an upper bound on front speed. The derivation starts by writing down a formal, implicit solution of equation (1) in terms of an average over trajectories of particles transported by the flow and subject to molecular diffusion [5]. Namely, we have

$$\theta(t, \mathbf{x}) = \left\langle \exp \left[\int_0^t \tau^{-1} c(\theta(s, \mathbf{r}(s))) ds \right] \theta(0, \mathbf{r}(0)) \right\rangle, \quad (2)$$

where $c(\theta)$ is the rate-of-growth of θ defined by $f(\theta) = c(\theta)\theta$. The trajectories evolve according to $\dot{\mathbf{r}} = \mathbf{v} + \sqrt{2\kappa}\boldsymbol{\eta}$ ($\boldsymbol{\eta}$ is the white noise term which accounts for molecular diffusion) and are subject to the final condition $\mathbf{r}(t) = \mathbf{x}$. The angular brackets $\langle \dots \rangle$ stand for the average over all realizations of the molecular noise $\boldsymbol{\eta}$. Due to the properties of $f(\theta)$, [3], the largest rate-of-growth occurs for $\theta = 0$, that is we have $c(\theta) \leq c(0) = f'(0) = 1$, which yields $\theta(t, \mathbf{x}) \leq \langle \theta(0, \mathbf{r}(0)) \rangle \exp(t/\tau)$. In the last expression, the term in angular brackets denotes the probability that the trajectory ending at \mathbf{x} were initially located at the left of the front interface. Under very broad conditions, i.e. nonzero molecular diffusivity and finite variance of the velocity vector potential [6–8], it is possible to show that asymptotically the particles undergo a normal diffusion process with an effective diffusion coefficient κ_{eff} , always larger than the molecular value κ . Consequently, we have $\theta(t, \mathbf{x}) \leq \exp[t/\tau - x^2/(4\kappa_{\text{eff}}t)]$, with exponential accuracy. We therefore obtain the upper bound for the front velocity,

$$v_{\text{eff}} \leq \sqrt{4\kappa_{\text{eff}}/\tau}. \quad (3)$$

It is worth remarking that the effective diffusivity itself is bounded by the relation $\kappa_{\text{eff}}/\kappa \leq 1 + \alpha Pe^2$, where α is a numerical constant that depends on the details of the flow [6–8]. This last relation along with (3) entail $v_{\text{eff}}/v \leq \sqrt{1 + \alpha Pe^2}$: in the limit of small Pe this bound is in agreement with the Clavin-Williams relation, [9], that describes the rate of convergence of v_{eff} to v for vanishing stirring intensity. On the contrary, the possibility

of small U asymptotics as $(v_{\text{eff}} - v)/v \sim U^{4/3}$, [10], is ruled out.

Until now we have not specified any detail of the velocity field. In many engineering applications \mathbf{u} is turbulent. Actually, it turns out that already the laminar cases are nontrivial, and moreover they show remarkable qualitative similarities with the turbulent case. In the context of laminar flows it is natural to consider two steady state configurations: an open flow field (shear flow), and a situation where all the streamlines are closed (convection rolls). The first case has been analyzed in detail in Refs. [11] and [12], with the main result that the effective front speed is proportional to the typical velocity of the advecting field. We will focus on the second situation, a flow made of an infinite sequence of steadily counter-rotating cells aligned along the horizontal direction. Here, we use as a model flow the incompressible two-dimensional velocity field $\mathbf{u} = (-\partial_y\psi, \partial_x\psi)$ generated by the streamfunction $\psi(x, y) = UL \sin(2\pi x/L) \sin(2\pi y/L)$ with L -periodic conditions in y and an infinite extent along the x -axis.

Does the bound (3) give a good estimate of the effective front speed for this problem? We performed numerical simulations of Eq. (1), [13], which show that in the regime $Da \ll 1$ the maximal front speed is indeed attained. Actually, when $Da \ll Pe^{-1}$ it is possible to prove, by means of homogenization techniques, that $v_{\text{eff}} = \sqrt{4\kappa_{\text{eff}}/\tau}$ [11]. On the contrary, at $Da \gg 1$ we observe a significative slow-down of the front speed signalled by a different scaling dependence on the parameters U, κ, L, τ (see Fig. 1).

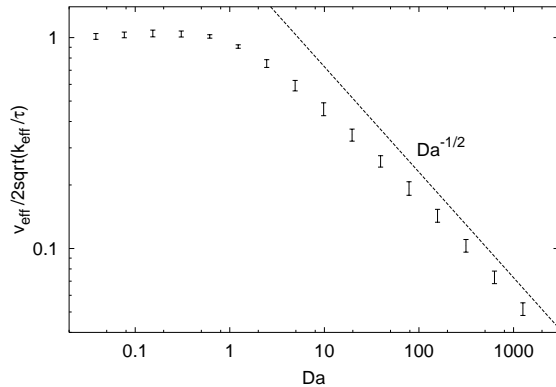


FIG. 1. The ratio of measured front speed, v_{eff} , to the maximal one, $\sqrt{4\kappa_{\text{eff}}/\tau}$, as a function of the Damköhler number, Da . For $Da \ll 1$ the front propagates with the maximal velocity whereas for $Da \gg 1$ the speed slows down with increasing Da . The behaviour $Da^{-1/2}$ is drawn for reference.

For a turbulent velocity field the experimental results are remarkably similar to the situation shown in Figure 1, with the only change that $\kappa_{\text{eff}} \sim U_T L_T$ where U_T is the typical turbulent intensity and L_T is the integral scale of turbulent motion [14]. The steady cellular

flow, notwithstanding its simplicity, provides thus for a powerful paradigm which can be insightful for the study of front propagation in turbulent flows.

The key to the understanding of the different regimes of front propagation stands in the description of front dynamics in terms of effective macroscopic equations, which we introduce hereafter. The dynamics of θ is characterized by the length-scale L , the cell-size. We can therefore perform a space discretization which reduces each cell, C_i , to a point, i , mapping the domain – a two-dimensional infinite strip – to a one-dimensional lattice, and the field θ to a function defined on the lattice $\Theta_i = L^{-2} \int_{C_i} \theta dx dy$. Integrating equation (1) over the cell C_i we obtain $\dot{\Theta}_i = J_{i+1} - J_i + \chi_i$ where $J_i = L^{-2} \int_{\text{left}} \kappa \partial_x \theta dy$ is the flux of matter through the left boundary of the i -th cell, and $\chi_i = L^{-2} \int_{C_i} \tau^{-1} f(\theta) dx dy$ is the rate of change of Θ_i due to reaction taking place within the cell. We will show that it is possible to model the dynamics with a space-discretized macroscopic reaction-diffusion equation:

$$\dot{\Theta}_i = \kappa_{\text{eff}} \left(\frac{1}{2} \Theta_{i+1} - \Theta_i + \frac{1}{2} \Theta_{i-1} \right) + \tau_{\text{eff}}^{-1} F(\Theta_i). \quad (4)$$

The effect of velocity is to *renormalize* the values of diffusivity, $\kappa \rightarrow \kappa_{\text{eff}}(\kappa, U, L)$, and reaction time-scale, $\tau \rightarrow \tau_{\text{eff}}(\tau, U, L)$ and therefore the advective term does not appear any longer in the effective dynamics Eq. (4) [15]. The renormalized diffusivity κ_{eff} accounts for the process of diffusion from cell to cell resulting from the nontrivial interaction of advection and molecular diffusion. The renormalized reaction-time τ_{eff} amounts to the time that it takes to a single cell to be completely burned, and depends on the interaction of advection and production. In that context, the limiting speed of the front in the moving medium will be $v_{\text{eff}} \sim \sqrt{\kappa_{\text{eff}}/\tau_{\text{eff}}}$. The goal is now to derive the expressions for the renormalized parameters from physical considerations.

Renormalization of diffusivity. To obtain the value of κ_{eff} it is sufficient to neglect the reaction term in equation (1), i.e. consider a passive scalar in a cellular flow. The solution is known, [16–18],

$$\frac{\kappa_{\text{eff}}}{\kappa} \sim Pe^{1/2} \quad Pe \gg 1. \quad (5)$$

For large Pe (κ small) the cell-to-cell diffusion mechanism can be qualitatively understood in the following way: the probability for a particle of scalar to jump across the boundary of the cell, in a circulation time L/U , by virtue of molecular diffusion, can be estimated as the ratio of the diffusive motion across streamlines, $O(\sqrt{\kappa L/U})$, to advective motion along streamlines, $O(L)$, leading to $p \sim (\kappa/(UL))^{1/2}$, hence the effective diffusivity $\kappa_{\text{eff}} \sim pUL \sim \kappa Pe^{1/2}$.

Renormalization of reaction time. At small Da , where reaction is significantly slower than advection, the cell is first invaded by a mixture of reactants and products

(with a low content of products, $\Theta_i \ll 1$) on the fast advective time-scale, and complete reaction ($\Theta_i = 1$) is then achieved on the slow time-scale $\tau_{\text{eff}} \simeq \tau$ (Figure 2). The area where the reaction takes place extends over several cells, i.e. the front is “distributed”.

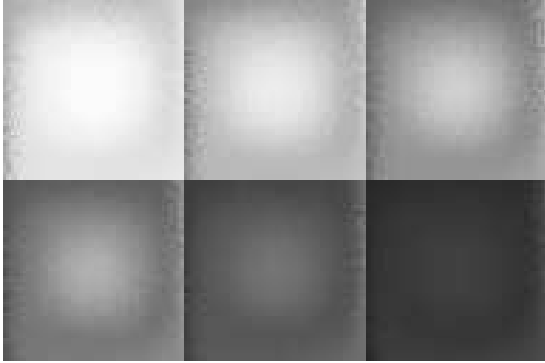


FIG. 2. Six snapshots of the field θ within a cell, at six successive times with a delay $\tau/6$ (from left to right, top to bottom), as a result of the numerical integration of equation (1). Here $Da \simeq 0.4$, $Pe \simeq 315$. Black stands for $\theta = 1$, white for $\theta = 0$.

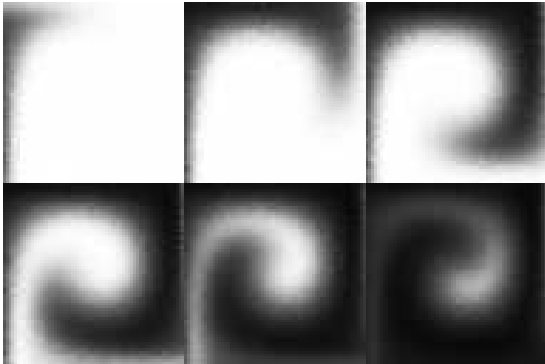


FIG. 3. Six snapshots of the field θ within a cell, at six successive times with a delay $(L/U)/6$ (left to right, top to bottom). Here $Da = 4$, $Pe = 315$. A spiral wave invades the interior of the cell, with a speed comparable to U .

At large Da , the ratio of time-scales reverses, and in a (now short) time τ two well-separated phases emerge inside the cell. The interface has a depth $\lambda \sim \sqrt{\kappa\tau} = LPe^{-1/2}Da^{-1/2}$, i.e. it is thin compared to the cell size. This is the so-called Huygens (or geometrical optics) limit for front propagation. Here the process is characterized by an inward spiral motion of the outer, stable phase (see Figure 3), at a speed proportional to U as it usually happens for a front in a shear flow at large Da . Indeed it is easy to show that, inside a cell, the problem can be mapped to a front propagation in a shear-flow in “action-angle” variables [19]. Therefore the $\theta = 1$ phase fills the whole cell on the advective time-scale, giving $\tau_{\text{eff}} \simeq L/U$. In summary, we have the following behavior for the renormalized reaction time

$$\frac{\tau_{\text{eff}}}{\tau} \sim \begin{cases} 1 & Da \ll 1 \\ Da & Da \gg 1. \end{cases} \quad (6)$$

Now, we have all the information to derive the effective speed of front propagation for a cellular flow. Recalling that $v_{\text{eff}} \sim \sqrt{\kappa_{\text{eff}}/\tau_{\text{eff}}}$, we have for the front velocity the final result

$$\frac{v_{\text{eff}}}{v} \sim \begin{cases} Pe^{1/4} & Da \ll 1, Pe \gg 1 \\ Pe^{1/4}Da^{-1/2} & Da \gg 1, Pe \gg 1 \end{cases} \quad (7)$$

where we restricted ourselves to the most interesting case $Pe \gg 1$. At small Da the front propagates with an effective velocity which scales as the upper bound derived above, that is as $Pe^{1/4}$. At large Da front speed is less enhanced than at small Da : according to Eq. (7), we have $v_{\text{eff}}/\sqrt{4\kappa_{\text{eff}}/\tau} \sim Da^{-1/2}$ for $Da \gg 1$. The results of numerical simulations confirm the above picture (see Figure 1). In terms of the typical velocity of the cellular flow, we have $v_{\text{eff}} \propto U^{1/4}$ for “fast” advection ($U \gg L/\tau$, or equivalently $Da \ll 1$) whereas $v_{\text{eff}} \propto U^{3/4}$ for “slow” advection ($U \ll L/\tau$, or $Da \gg 1$). The numerical results are shown in Figure 4.

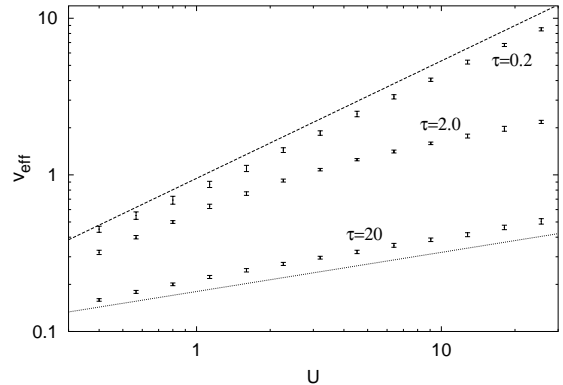


FIG. 4. The front speed v_{eff} as a function of U , the typical flow velocity. The lower curve shows data at $\tau = 20.0$ (fast advection). The intermediate curve at $\tau = 2.0$ shows the crossover from fast (right side) to slow advection (left side) that takes place at $U \sim L/\tau$. The upper curve shows data at $\tau = 0.2$ (slow advection). For comparison, the scalings $U^{1/4}$ and $U^{3/4}$ are shown as continuous lines.

In the geometrical optics limit $Da \gg 1$, $Pe \gg 1$, the effective speed of the front is proportional to the area of the interface that separates the two phases. In two dimensions, the interface is characterized by its length, ℓ , and its depth, λ . We have the relationship $v_{\text{eff}} \sim \lambda\ell/(L\tau)$ which entails the result that the ratio of the length of the interface in a moving medium, ℓ , to the length in a medium at rest, L , is $\ell/L \sim v_{\text{eff}}/v$ and is therefore larger than unity. The structure responsible for this elongation of the front edge is the spiral wave shown in Figure 3. Finally, it is interesting to look at the shape of the effec-

tive reaction term $\tau_{\text{eff}}^{-1}F(\Theta)$ appearing in the renormalized equation (4). As shown in Figure 5, for small Da the effective production term is indistinguishable from the “bare” one. Increasing Da , the reaction rate tends to reduce progressively, inducing the slow-down of the front speed. The effective potential shows a small region where the production term is essentially the microscopic one, followed by an intermediate regime characterized by a linear dependence on the cell-averaged concentration, with a slope directly proportional to Da^{-1} . That is in agreement with a typical effective reaction time $\tau_{\text{eff}} \sim \tau Da$ (cf. eq. (6)).

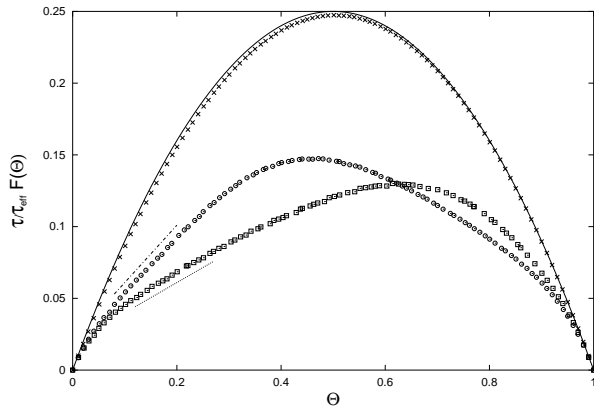


FIG. 5. The renormalized reaction term $\tau/\tau_{\text{eff}}F(\Theta)$ for three different parameter: $Da \simeq 4$ (\square), $Da \simeq 2$ (\circ) and $Da \simeq 0.4$ (\times). The continuous line is $f(\theta)$. The dotted and dash-dotted lines are the slopes (0.2 and 0.4) proportional to Da^{-1} in the region of slow advection.

Notwithstanding the change of shape of the effective chemical potential due to advection, the production term remains in the universality class of KPP-type. What happens if the microscopic reaction term is of Arrhenius-type? For shear flows, it is known that quenching takes place for most of velocity profiles, [20], with the result that the effective reaction term is identically renormalized to zero. Which are the general conditions for quenching in arbitrary, possibly turbulent flow? This problem represents one of the challenges for future research on front propagation.

We acknowledge several stimulating discussions with R. M. McLaughlin, A. Pumir and M. Vergassola. This work has been partially supported by the INFM *Parallel Computing Initiative* and MURST (Cofinanziamento *Fisica Statistica e Teoria della Materia Condensata*). M.A. is supported by the European Network *Intermittency in Turbulent Systems* (FMRX-CT98-0175).

- [1] F. A. Williams, *Combustion Theory*, Benjamin-Cummings, Menlo Park (1985); E. R. Abraham, *Nature* **391**, 577 (1998); I. R. Epstein, *Nature* **374**, 231 (1998); J. Ross, S. C. Müller, and C. Vidal, *Science* **240**, 460 (1988).
- [2] Here we assume that the velocity field is given, and that the concentration of chemicals does not affect the hydrodynamics. In that sense, concentration is a passive, albeit reactive, scalar. This approximation is hardly tenable in the context of flame propagation in gases, but it appears quite reasonable for chemical front propagation in aqueous solutions (see Ref. [14]).
- [3] The function $f(\theta)$ is concave and positive in the interval $(0, 1)$, vanishing at its extremes, and $f'(0) = 1$. These conditions define a KPP-type production term. Other choices are possible, namely an Arrhenius law, more appropriate to the study of flames and/or chemical reactions, but the discussion here will limit to a KPP-type term. The domain is a two-dimensional strip of height L and infinite extent in the horizontal direction. The initial condition is defined by $\theta = 1$ on the left side of the domain, and $\theta = 0$ on the right side. The maximum principle ensures that at later times the field still takes values in the range $0 \leq \theta \leq 1$. The front speed is defined as $L^{-1} \int \partial_t \theta dx dy$.
- [4] A. N. Kolmogorov, I. G. Petrovskii, and N. S. Piskunov, *Moscow Univ. Bull. Math.* **1**, 1 (1937).
- [5] M. Freidlin, *Markov Processes and Differential Equations* Birkhauser, Boston (1996).
- [6] M. Avellaneda, and A. Majda, *Phys. Rev. Lett* **62**, 753 (1989).
- [7] M. Avellaneda and M. Vergassola *Phys. Rev. E* **52**, 3249 (1995).
- [8] R. H. Kraichnan, in *The Padé Approximants in Theoretical Physics*, Acad. Press Inc., New York (1970).
- [9] P. Clavin, and F. A. Williams, *J. Fluid Mech.* **90**, 589 (1979).
- [10] A. R. Kerstein, and W. T. Ashurst, *Phys. Rev. Lett* **68**, 934 (1992).
- [11] P. Constantin, A. Kiselev, A. Oberman, and L. Ryzhik, LANL e-print archive math/9907132 (1999).
- [12] B. Audoly, H. Berestycki and Y. Pomeau *C. R. Acad. Sci.* **328**, Série II b, 255 (2000).
- [13] The numerical method is a Montecarlo simulation of the (time-discretized) path integral appearing in Equation (2). Further details will be reported elsewhere.
- [14] P. D. Ronney, B. D. Haslam and N. O. Rhys, *Phys. Rev. Lett.* **74**, 3804 (1995).
- [15] The assumption that κ and τ are independently renormalized by advection is consistent in the regime $v/U = (Da/Pe)^{1/2} \ll 1$.
- [16] M. N. Rosenbluth, A. L. Berk, I. Doxas, and W. Horton, *Phys. Fluids* **30**, 2636 (1987).
- [17] B. I. Shraiman, *Phys. Rev. A* **36**, 261 (1987).
- [18] Y. Pomeau *C. R. Acad. Sci.* **301** 1323 (1985).
- [19] P. B. Rhines and W. R. Young, *J. Fluid Mech.* **133**, 133 (1983).
- [20] P. Constantin, A. Kiselev & L. Ryzhik, LANL e-print archive nlin/0006024 (2000).